POMC neurons control fertility through differential signaling of MC4R in Kisspeptin neurons in the female mouse

Authors:
Rajae Talbi[1,2*], Todd L. Stincic[4,*#], Kaitlin Ferrari[2], Choi Ji Hae[2], Karol Walec[2,] Elizabeth Medve[2], Achi Gerutshang[2], Silvia León[1,2], Elizabeth A. McCarthy[1,2], Oline K. Rønnekleiv [4,5], Martin J. Kelly[4,5] and Víctor M. Navarro[1,2,6]

[1]Harvard Medical School, Boston, MA, USA; [2]Division of Endocrinology, Diabetes and Hypertension, Department of Medicine, Brigham and Women's Hospital, Boston, MA, USA; [4]Department of Chemical Physiology and Biochemistry, Oregon Health & Science University, Portland, OR, USA; [5]Division of Neuroscience, Oregon National Primate Research Center, Beaverton, OR, USA; [6]Harvard Program in Neuroscience, Boston, MA, USA

*First authors contributed equally
[#]Present address: Department of Biology, Appalachian State University, Boone, NC 28608.

Correspondence:
Victor M. Navarro, PhD, Division of Endocrinology, Diabetes and Hypertension, Department of Medicine, Brigham and Women's Hospital and Harvard Medical School, 221 Longwood Avenue, Room 219, Boston, Massachusetts 02115. E-mail: vnavarro@bwh.harvard.edu.

Martin J. Kelly, PhD, Department of Chemical Physiology and Biochemistry, Oregon Health & Science University, 3181 SW Sam Jackson Park Road, Portland, OR 97239. E-mail: kellym@ohsu.edu .

Authors contribution: RT, TLS, MJK and VMN conceived and designed the study; RT, TLS, KF, CJH, EM, AG, KW, SL, EAM, OKR performed the experiments. RT, TLS, OKR, MJK and VMN analyzed data. RT, TLS and VMN wrote the manuscript with input from all the authors.

Competing Interests Statement: The authors declare they have no competing interest.

Data and Materials Availability: All data needed to evaluate the conclusions in the paper are present in the paper and/or the Supplementary Materials.

Keywords: Kiss1 neurons, MC4R, POMC, Fertility, Obesity

Abstract

Inactivating mutations in the melanocortin 4 receptor (*MC4R*) gene cause monogenic obesity. Interestingly, female patients also display various degrees of reproductive disorders, in line with the subfertile phenotype of MC4RKO female mice. However, the cellular mechanisms by which MC4R regulates reproduction are unknown. Kiss1 neurons directly stimulate gonadotropin-releasing hormone (GnRH) release through two distinct populations; the Kiss1^{ARH} neurons, controlling GnRH pulses, and the sexually dimorphic Kiss1$^{AVPV/PeN}$ neurons controlling the preovulatory LH surge driving ovulation. In the present study, we show that *Mc4r* is expressed within Kiss1^{ARH} and Kiss1$^{AVPV/PeN}$ neurons. *In vivo*, deletion of MC4R from Kiss1 neurons in female mice replicates the reproductive impairments of MC4RKO mice without inducing obesity. Conversely, reinsertion of MC4R in Kiss1 neurons of MC4R null mice restores estrous cyclicity and LH pulsatility without reducing their obese phenotype. *In vitro*, we show that MC4R activation excites Kiss1^{ARH} neurons through direct synaptic actions. In contrast, Kiss1$^{AVPV/PeN}$ neurons are normally inhibited by MC4R activation except under elevated estradiol levels, thus facilitating the activation of Kiss1$^{AVPV/PeN}$ neurons to induce the preovulatory LH surge driving ovulation in females. Our findings demonstrate that POMC^{ARH} neurons acting through MC4R, directly regulate reproductive function in females by stimulating the “pulse generator” activity of Kiss1^{ARH} neurons and restricting the activation of Kiss1$^{AVPV/PeN}$ neurons to the time of the estradiol-dependent LH surge, and thus unveil a novel pathway of metabolic regulation of fertility.

Significance:

Women with inactivating mutations in proopiomelanocortin (*POMC*) or melanocortin receptor 4 (*MC4R*) genes are severely obese and display various degrees of reproductive disorders; however, the mechanisms by which MC4R regulates reproduction remain unknown. Here, we show that the melanocortins, known for their fundamental role in the control of energy balance, also play a direct role in reproduction by modulating the tonic and surge-like release of GnRH/LH via direct actions on MC4R of Kiss1 neurons. These findings identify a direct link between the neural regulation of metabolism and fertility and offer a new platform for the development of novel approaches to treat reproductive deficiencies derived from metabolic impairments.

Introduction

Obesity rates have skyrocketed in Western societies in the last decades, resulting in an alarming rise in comorbidities that place a significant burden on healthcare systems. The increase in obesity correlates with a decrease in fertility rates, leading to conception challenges that are experienced by approximately 15% of couples in the United States currently (1).

The melanocortin receptor 4 (MC4R) binds α-melanocyte stimulating hormone (αMSH), an agonist product of the pro-opiomelanocortin (*Pomc*) gene, and the inverse agonist of the agouti-related peptide (AgRP) to regulate food intake and energy expenditure (2, 3). While the role of MC4R on food intake is largely mediated by neurons located in the paraventricular nucleus of the hypothalamus (PVN) (4), its expression in the brain is widespread (5) with the specific function of the different MC4R-expressing neurons in areas beyond the PVN remaining to be fully explored. Inactivating mutations in *MC4R* are a leading cause of monogenic obesity in humans and mice (6). Scant evidence in humans shows an association between *MC4R* mutations and higher incidence of hypogonadotropic hypogonadism (HH) (7), alterations in the timing of puberty onset (8), and polycystic ovary syndrome (PCOS) (9); however, conflicting reports exist (6). Therefore, the role of MC4R signaling in reproductive function in humans remains controversial despite the clear association found in mice. Supporting this role of MC4R, *Mc4r* null mice display an array of reproductive abnormalities that largely affects females, characterized by irregular estrous cycles, disrupted luteinizing hormone (LH) secretion, reduced corpora lutea and reduced fertility (10-12). Further evidence from mice demonstrates that MC4R agonists robustly increase LH release in a kisspeptin-dependent manner (13).

Kisspeptin is the most potent gonadotropin releasing hormone (GnRH) secretagogue known to date and it is mainly produced in two distinct neuronal populations. Kiss1 neurons of the arcuate nucleus ($Kiss1^{ARH}$) neurons control the pulsatile (tonic) release of GnRH (present in both sexes), and sex steroids attenuate their release of kisspeptin. However, while testosterone inhibits

139 Kiss1^{ARH} glutamate release (14), estradiol enhances the vesicular-glutamate transporter 2
140 (*Vglut2)* expression and glutamate release probability which could reflect changing roles of
141 Kiss1^{ARH} neurons across the estrous cycle (15). Kiss1 neurons of the anteroventral periventricular
142 continuum area (Kiss1$^{AVPV/PeN}$), which are predominantly present in females, are responsible for
143 generating the preovulatory GnRH/LH surge (16). Despite these critical roles of both populations
144 of Kiss1 neurons for reproduction, the underlying mechanisms that determine how each Kiss1
145 population responds differently to sex steroids remains unresolved. Fibers from POMC neurons
146 in the arcuate nucleus (POMC^{ARH}) project to and juxtapose Kiss1^{ARH} neurons (13); and
147 melanocortin signaling through MC4R contributes to the permissive role of leptin on puberty onset
148 (13, 17, 18). Altogether, the existing data in rodents suggests a clear role for MC4R, likely on
149 Kiss1 neurons, in the control of reproductive maturation and fertility.
150 In this study, we investigated the contribution of MC4R signaling versus obesity per se in the
151 etiology of the reproductive impairments observed in *Mc4r* null mice, which could explain similar
152 impairments observed in humans.
153

154 ## Results

155 ***Mc4r* is expressed within Kiss1 neurons and determines the timing of puberty onset in**
156 **females.**
157 As the expression of *Mc4r* in Kiss1 neurons has been inconclusive in previous studies, we began
158 by using the highly sensitive RNAscope *in situ* hybridization method. Dual fluorescence labeling
159 of *Mc4r* and *Kiss1* probes showed that 84% of Kiss1^{ARH} neurons and 74% of Kiss1$^{AVPV/PeN}$ neurons
160 expressed *Mcr4* (**Fig. 1*A, B***). To further investigate the specific role of MC4R in Kiss1 neurons,
161 we generated a Kiss1-specific MC4R knockout model (Kiss1-MC4RKO). The specific deletion of
162 *Mc4r* from Kiss1 neurons, as well as the absence of global recombination, were confirmed through
163 RNAscope. While Kiss1 neurons of Kiss1-MC4RKO mice lack *Mc4r* transcript compared to their

164 control littermates (**Fig. S*1A***), *Mc4r* was detectable in the PVN of all mice, which is a major site
165 of *Mc4r* expression in the brain, therefore supporting the specific deletion of *Mc4r* only within
166 Kiss1 neurons (**Fig. S*1B***).
167 Puberty onset was assessed daily from weaning age through the monitoring of vaginal opening
168 (VO) and first estrus (FE). Kiss1-MC4RKO females showed a significant advancement in the age
169 of VO (P=0.0150, Kiss1-MC4RKO: 24.67± 0.3978 vs controls: 26.32±0.5301) and FE (P=0.0341,
170 Kiss1-MC4RKO: 32.63±1.489 vs controls: 37.84±1.903) compared to their littermate controls
171 (**Fig. 1*C, D***). Body weight of Kiss1-MC4RKO females at the age of puberty onset was similar
172 between groups (P=0.2596, Kiss1-MC4RKO: 12.41±0.3041 vs controls: 12.89±0.2631) (**Fig. 1*E***).
173 These data suggest that melanocortin signaling on Kiss1 neurons participates in the timing of
174 puberty onset in females. Since the role of the melanocortin system on puberty onset is largely
175 unexplored, we evaluated the expression profile of the main components of this system in the
176 hypothalami of female mice at postnatal days (PND) 10, 15, 22 and 30. Interestingly, expressions
177 of *Agrp*, *Mc3r* and *Mc4r* were significantly lower at the time of puberty onset (PND30) in Kiss1-
178 MC4RKO females compared to earlier developmental ages (**Fig. 1*F***). This suggests that a
179 decrease in the hypothalamic melanocortin tone drives puberty onset, in line with the
180 advancement in the age of VO and FE observed in Kiss1-MC4RKO female mice (**Fig. 1*C, D***).
181
182 **MC4R in Kiss1 neurons is required for female reproduction.**
183 Because Kiss1-MC4RKO females showed altered puberty onset, we further investigated their
184 reproductive phenotype. Interestingly, Kiss1-MC4RKO female mice displayed normal BW
185 throughout the time of the study (up to PND150) **(Fig. 2*A*)**; however, they presented with irregular
186 estrous cycles with predominantly more time spent in diestrus (P=0.0001) and less time spent in
187 estrus (P<0.0001) than their control littermates (**Fig. 2*B, C***). The assessment of the pulsatile
188 release of LH every 10 min over 180 min revealed no change in the total number of pulses
189 between groups but a significant increase in basal LH release (P=0.0368) in Kiss1-MC4RKO

190 female mice (0.426±0.036) compared to controls (0.339±0.026) (**Fig. 2*D-H***). The analysis of the
191 gene expression of the "KNDy" systems in the ARH, which control the GnRH pulse generator
192 (16), revealed normal expression levels of *Kiss1*, *Tac2* and *Tacr3*, but significantly lower
193 expression of *Pdyn* (P=0.0067, Kiss1-MC4RKO: 0.781±0.0384 vs controls: 1.000±0.0190) (**Fig.**
194 **2*I-L***). The conserved expression of *Kiss1*, *Tac2* and *Tacr3* correlates with the preserved LH pulse
195 frequency and amplitude in Kiss1-MC4RKO mice, while the lower inhibitory tone of dynorphin
196 (**Fig. 2*I***) correlates with the higher basal LH levels (**Fig. 2*G***). To assess the contribution of MC4R
197 signaling in Kiss1 neurons to the induction of the preovulatory LH surge, Kiss1-MC4RKO females
198 and control littermates were submitted to an LH surge induction protocol that showed the LH
199 surge was significantly blunted in the Kiss1-MC4RKO females (P=0.0091), while the protocol
200 clearly evoked the expected afternoon rise of LH in control mice (**Fig. 2*M***). In line with these
201 findings, the ovaries of Kiss1-MC4RKO females displayed fewer corpora lutea (P=0.0054, Kiss1-
202 MC4RKO: 0.800±0.374 vs controls: 2.80±0.374) and increased cystic follicles (P=0.0337, Kiss1-
203 MC4RKO: 1.60±0.400 vs controls: 0.400±0.244) (**Fig. 2*N-P***), which correlate with decreased
204 fertility as observed by the extended time to deliver pups (*i.e.* longer time to get pregnant)
205 (P=0.0030, Kiss1-MC4RKO: 30.30±4.600 vs controls: 20.88±0.2266), and fewer pups per litter
206 (P=0.0095, Kiss1-MC4RKO: 6.667±0.5528 vs controls: 8.444±0.242) (**Fig. 2*S, T***).
207 The increase in serum LH levels and decreased ovulation observed in the Kiss1-MC4RKO
208 females is reminiscent of polycystic ovary syndrome (PCOS) mouse models (19, 20). Thus, we
209 analyzed circulating levels of testosterone (T) and anti-müllerian hormone (AMH), which are
210 frequently elevated in PCOS models (21). The Kiss1-MC4RKO females expressed normal T and
211 AMH levels compared to control mice in diestrus (**Fig. 2*Q, R***). Thus, we can exclude a PCOS-like
212 reproductive phenotype mediated by the lack of melanocortin signaling on Kiss1 neurons.
213
214
215

216 **Re-insertion of MC4R in Kiss1 neurons of MC4RKO mice improves reproductive function.**
217 Kiss1-MC4RKO females displayed reproductive abnormalities resembling those described in
218 MC4RKO females (10-12). Thus, we hypothesized that the reproductive defects described for the
219 MC4RKO mice would be, at least in part, due to the absence of MC4R signaling in Kiss1 neurons.
220 To further investigate this hypothesis, we generated mice that do not express *Mc4r* anywhere
221 (MC4R-LoxTB, *i.e.* MC4RKO) or that express *Mc4r* only in Kiss1 neurons (*Kiss1-cre:MC4R-*
222 *loxTB*). The re-insertion of *Mc4r* within Kiss1 neurons in the *Kiss1-cre:MC4R-loxTB* mice was
223 confirmed through RNAscope (**Fig. S2*A*).** *Mc4r* expression was not detected in the PVN of these
224 mice (**Fig. S2*B***), and it was only detected in Kiss1 neurons in the *Kiss1-cre:MC4R-loxTB* mice.
225 Puberty onset was assessed daily from weaning age through the monitoring of vaginal opening
226 (VO) and first estrus (FE). MC4R-LoxTB and *Kiss1-cre:MC4R-loxTB* female mice displayed
227 normal timing of puberty onset compared to their control littermates, as assessed by VO (P=0.104,
228 MC4R-LoxTB: 30.86±1.908 vs *Kiss1-cre:MC4R-loxTB: 30.09*±1.004 vs controls: 27.57±0.8168),
229 and FE (P=0.8472, MC4R-LoxTB: 35.14±2.463 vs *Kiss1-cre:MC4R-loxTB: 34.55*±1.648 vs
230 controls: 35.80±0.8406) (**Fig. 3*A***), despite displaying significantly higher body weight at the time
231 of puberty onset (P=0.0001, MC4R-LoxTB: 15.49±0.5078 vs *Kiss1-cre:MC4R-loxTB:* 15.54±0.40
232 vs Controls: 13.29±0.30) (**Fig. 3*B***). As expected, MC4R-LoxTB (MC4RKO) displayed increased
233 body weight (**Fig. 3C**) and an array of reproductive impairments that included: irregular estrous
234 cycles with significantly more days in diestrus (P=0.0016) and fewer days in estrus (P=0.0317)
235 compared to controls (**Fig. 3*D, E***), significantly higher serum LH levels characterized by higher
236 basal (P=0.0882, MC4R-LoxTB: 0.48±0.02 vs Controls: 0.37±0.06) and amplitude levels per LH
237 pulse (P=0.0102, MC4R-LoxTB: 0.73±0.009 vs Controls: 0.58±0.07) despite unaltered number of
238 LH pulses/180min (P=0.2285, MC4R-LoxTB: 2.00±0.40 vs Controls: 3.50±0.50) (**Fig. 3*F-J***), and
239 fewer corporal lutea (P=0.0366, MC4R-LoxTB: 0.80±0.80 vs Controls: 4.20±1.15) (**Fig. 3*K, L***),
240 recapitulating the same reproductive phenotype observed in Kiss1-MC4RKO mice despite the
241 differences in BW. Re-introduction of MC4R into Kiss1 neurons in *Kiss1-cre:MC4R-loxTB* mice

242 completely recovered estrous cyclicity, which was similar to controls (diestrus: P=0.1932,
243 proestrus: P=0.8262, estrus: P=0.0547, compared to controls) (**Fig. 3*D, E***) despite *Kiss1-*
244 *cre:MC4R-loxTB* mice showing the same degree of obesity as MC4R-LoxTB mice (**Fig. 3*C***),
245 indicating that obesity *per se* was not mediating the irregular estrous cycles in MC4RKO mice. As
246 indicated above, MC4R-LoxTB mice display higher overall circulating LH levels, and this feature
247 was also recovered by the insertion of MC4R in Kiss1 neurons of *Kiss1-cre:MC4R-loxTB* mice
248 (basal LH: 0.32±0.044, LH amplitude: 0.48±0.04, LH pulses/180min: 2.40±0.67 and AUC:
249 70.62±7.156 compared to controls: 80.36±9.058 compared to controls) (**Fig. 3*G-I***), further
250 confirming that melanocortin action on Kiss1 neurons is required for the normal control of
251 gonadotropin release. Despite these significant improvements in reproductive function, *Kiss1-*
252 *cre:MC4R-loxTB* mice presented fewer corpora lutea than controls (0.80±0.80), similar to MC4R-
253 LoxTB mice, suggesting that an ovulatory impairment still persists (**Fig. 3*K, L***). While tonic LH
254 release and estrous cyclicity are predominantly controlled by Kiss1^{ARH} neurons, ovulation is
255 mediated by the induction of the preovulatory LH surge by Kiss1$^{AVPV/PeN}$ neurons. It is possible
256 that the metabolic signals derived from their obese phenotype, and/or the absence of the direct
257 action of MC4R in GnRH neurons (17, 22) prevents the complete recovery of ovulation in *Kiss1-*
258 *cre:MC4R-loxTB* mice. Both genetic models displayed significantly lower T (MC4R-LoxTB:
259 28.50±6.20 vs *Kiss1-cre:MC4R-loxTB:* 31.22±3.90 vs Controls: 62.84±16.53) and AMH (MC4R-
260 LoxTB: 150.6±22.00 vs *Kiss1-cre:MC4R-loxTB:* 146.9±10.83 vs Controls: 321.8±15.70) levels
261 than control mice in diestrus (**Fig. 3*M, N***). Therefore, we can exclude a PCOS-like reproductive
262 phenotype mediated by the lack of melanocortin signaling.
263

264 **Kiss1^{ARH} neurons are excited by MC4R agonists.**

265 Based on the RNAscope and reproductive phenotype data, we hypothesized that Kiss1^{ARH}
266 neurons are direct targets of melanocortins and would respond to MC4R activation. Initially we
267 did whole-cell, voltage clamp recordings in Kiss1^{ARH} neurons (**Fig. 4*A***). *Kiss1-Cre* x Ai32 or *Kiss1-*

268 *Cre* AAV-injected mice underwent OVX and were given E2 replacement (see Methods). We
269 targeted fluorescent cells for recording which were isolated synaptically by bathing the slices in
270 tetrodotoxin (TTX, 1 μM). Focal application of the high-affinity melanocortin receptor agonist
271 melanotan II (MTII, ~250 nM) elicited a small inward current in half of the isolated Kiss1^{ARH} cells
272 (10/21) (**Fig. 4*B***). Next, we examined if the E2 state affected MTII response by recording from
273 Kiss1^{ARH} neurons from OVX females and found two thirds (6/9 cells) responded, but there was no
274 significant difference in the average current (**Fig. 4*C***). Finally, it must be noted that at this
275 concentration MTII is a non-selective MCR agonist, so we followed up using a perfusion of the
276 MC4R-selective agonist THIQ (100 nM) to determine if activation of MC4Rs alone was sufficient
277 to invoke a postsynaptic response in Kiss1^{ARH} neurons from OVX+E2 females. Similar to MTII,
278 THIQ was able to elicit an excitatory inward current in Kiss1^{ARH} neurons (4/5 cells, -7.4±0.5 pA),
279 indicating MC4R activation is sufficient (**Fig. 4*D***).
280
281 **POMC neurons synapse directly with Kiss1^{ARH} neurons.**
282 Based on the pharmacological activation of MCRs, we wanted to address whether POMC^{ARH}
283 neurons are the source of melanocortins to excite Kiss1^{ARH} neurons directly. To answer this
284 question, we injected an AAV-EF1α-DIO-ChR2:mCherry vector into the ARH of adult *Pomc-Cre*
285 female mice (**Fig. 4*E***) (24). After 2-4 weeks we did whole cell recordings from putative Kiss1^{ARH}
286 neurons and looked for a response to high frequency optogenetic stimulation of POMC fibers in
287 OVX + E2-treated females (**Fig. 4*F***). We were able to confirm that these were Kiss1 neurons
288 based on the presence of a persistent sodium current and/or *post hoc* identification by scRT-PCR
289 (41/69 cells, **Fig. 4*G***). While this current is more prevalent in the AVPV Kiss1 population, Kiss1
290 neurons are the only ARH neurons to display this electrophysiological "fingerprint" of a
291 pronounced INaP paired with a high capacitance and low input resistance (23). Additionally, while
292 recording from putative Kiss1^{ARH} neurons, we optogenetically stimulated POMC fibers at low
293 frequency (1 Hz, 5 ms, 470 nm light) and recorded fast postsynaptic inward currents. The fast

294 kinetics of the EPSC are also a tell-tale sign of an ionotropic glutamatergic response (24).
295 Previously, CNQX was sufficient to block similar excitatory ESPCs in other postsynaptic targets
296 of POMC neurons (25). While the consistent latency from optogenetic stimulus and current
297 response was indicative of a single synaptic delay, we wanted to establish that it was a direct
298 synaptic connection, as we have previously shown for output of POMC neurons (25) and Kiss1
299 neurons (26-28). First, we abrogated the optogenetic response with the addition of TTX (1 μM)
300 to the bath, we were able to rescue the postsynaptic glutamate response with the addition of the
301 K^+ channel blockers 4-aminopyridine (4-AP; 0.5 mM) and tetraethyl ammonium (TEA; 7.5 mM)
302 (**Fig. 4*H***). K+ channel block enables the calcium inflow from ChR2 in the presynaptic terminals
303 to be sufficient to restore vesicle fusion. Therefore, there appears to be no intervening synapses
304 between POMC and the downstream $Kiss1^{ARH}$ neurons.
305 Previously we found that E2 increases glutamate release from POMC neurons by increasing
306 *Vglut2* (25). Therefore, we compared the postsynaptic glutamatergic responses following two
307 optogenetic stimuli (50 ms interval between light flashes) in $Kiss1^{ARH}$ neurons from OVX + vehicle
308 versus OVX + E2-treated female mice (**Fig. 4*I***). As anticipated, we found that treatment with E2
309 increased the probability of glutamate release from POMC neurons onto $Kiss1^{ARH}$ neurons based
310 on the significant decrease in the paired pulse ratio of the two stimuli (29) (**Fig. 4*J***). Although in
311 the present study we used an *in vivo* treatment paradigm, we know from previous studies that this
312 augmentation of glutamate release can happen quite rapidly after a brief exposure to E2 *in vitro*
313 (within 15 min) (25). Therefore, $Kiss1^{ARH}$ neurons are excited by the glutamatergic input from
314 POMC neurons in an E2-dependent manner.
315 Finally, given that POMC neurons project directly onto $Kiss1^{ARH}$ neurons, we wanted to show that
316 the evoked slow inward current with high frequency stimulation was mediated by αMSH. Indeed,
317 high frequency stimulation evoked an excitatory inward current (**Fig. 4*K***) that was blocked by the
318 selective MC3/4R antagonist SHU 9119 (**Fig. 4*L***). The number of high frequency (peptidergic)
319 responses seen in Kiss1 neurons that displayed low frequency postsynaptic (glutamatergic)

320 currents was low (4/16, 25%, mean inward current: -1.4±3.1 pA). However, since these recordings
321 were made in brain slices from E2-treated, OVX females and β-endorphin expression is enhanced
322 by E2 treatment (30), we were concerned that co-release of the opioid peptide could obscure
323 melanocortin postsynaptic effects. Indeed, there was a notable increase in slow inward currents
324 generated by high frequency stimulation of POMC fibers in slices that were perfused with the non-
325 selective opioid antagonist naloxone (1 μM) (9/23, 40%, mean inward current: -7.6±2.9 pA) (**Fig.**
326 ***4M***).
327 Together these optogenetic findings reinforced our pharmacological results showing that Kiss1^{ARH}
328 neurons are excited by MTII, and THIQ. Additional studies would need to be done to identify the
329 cation conductance that is affected by the MC4R signaling cascade in Kiss1^{ARH} neurons, but
330 clearly we have established that there are excitatory glutamatergic and peptidergic inputs from
331 POMC to Kiss1^{ARH} neurons.
332
333 **Kiss1$^{AVPV/PeN}$ neurons are inhibited by MC4R agonists.**
334 Having established a direct, excitatory projection from POMC to Kiss1^{ARH} neurons, we next
335 examined POMC inputs to Kiss1^{AVPVPeN} neurons. First, we used immunocytochemistry to label
336 fibers expressing αMSH to demonstrate that POMC fibers densely innervated the AVPV/ PeN
337 area (**Fig. 5*A***). We hypothesized that Kiss1$^{AVPV/PeN}$ neurons would be excited by exogenous
338 application of melanocortins because the receptor is typically Gs-coupled (31, 32). We did whole-
339 cell, voltage clamp recordings from Kiss1$^{AVPV/PeN}$-Cre::Ai32 neurons, which were isolated
340 synaptically by bathing the neurons in TTX (1 μM), from OVX females. For these experiments,
341 we tested the response to the high affinity melanocortin receptor agonist MTII (500 nM).
342 Surprisingly, we consistently measured an outward (inhibitory) current that could be reversed on
343 washout of MTII (**Fig. 5*B***). This outward current was associated with an increase in a K^+
344 conductance based on the current-voltage plot *(i.e.,* the outward current reversed at ~E_{K+}, **Fig.**
345 **5C**). Also, the inwardly-rectifying I/V could indicate that MC4R is coupled to activation of inwardly-

346 rectifying K^+ channels as has been previously reported for MC4R signaling in pre-autonomic
347 parasympathetic neurons in the brainstem (33). We hypothesized that the coupling could be
348 modulated by E2 via a $G\alpha_q$-coupled membrane estrogen receptor (Gq-mER) as we have
349 previously demonstrated in POMC neurons (34-36). For these experiments, we again utilized
350 OVX females and targeted Kiss1$^{AVPV/PeN}$-Cre::Ai32 neurons. Once in the whole-cell voltage-clamp
351 configuration, we perfused the slices with STX (10 nM), a selective ligand for the putative Gq-
352 mER (36), and tested the response to the MTII. Indeed, the outward current (inhibitory) response
353 to MTII was completely abrogated and even reversed by STX (**Fig. 5*D, E***). The short-term (bath)
354 treatment with STX ensured that there was no desensitization of the Gq-mER with longer-term (*in*
355 *vivo*) treatment with E2. Therefore, estrogen receptor activation can rapidly uncouple (*i.e.,*
356 desensitize) the MC4R inhibitory response in Kiss1$^{AVPV/PeN}$ neurons. We would predict that the
357 intracellular signaling cascade for the heterologous desensitization is similar to what we have
358 elucidated in POMC neurons (36), but this will need to be determined in future experiments. We
359 next investigated the response in vehicle-treated, OVX females. Indeed, Kiss1$^{AVPV/PeN}$ neurons
360 were even more inhibited by the same MTII exposure (**Fig. 5*E***). Therefore, in contrast to Kiss1^{ARH}
361 neurons, the MC4R appears to be coupled to opening of K^+ channels in Kiss1$^{AVPV/PeN}$ neurons. To
362 further establish whether the MTII was having pre- or postsynaptic effects, we measured the
363 glutamatergic mEPSCs before and after melanocortin receptor activation. We found there was no
364 significant effect on the frequency (**Fig. 5F**), but there was an effect on the amplitude (**Fig. 5G**).
365 This further supports a postsynaptic locus of STX's effects. However, *posthoc* comparisons found
366 STX increased amplitude compared to both OVX and OVX+E. This result hints at a membrane
367 delimited effect as STX is a much more potent agonist for Gq-mER than E2 (37).
368

369 ## Discussion

370 Our findings show that melanocortins act directly on Kiss1 neurons to contribute to the metabolic
371 regulation of fertility, in line with previous reports showing that αMSH stimulates LH release in a

372 kisspeptin-dependent manner (13). Several studies in humans have linked *MC4R* mutations to
373 reproductive abnormalities, including precocious puberty (8), PCOS (9), and hypogonadism (7).
374 However, a direct association between *MC4R* mutations and reproductive function, independent
375 from the obese condition of these patients, has not been identified (6). In the current study, we
376 demonstrate that the majority of Kiss1 neurons express the *Mc4r* transcript, and we show that the
377 reproductive impairments observed in MC4R deficient mice, which replicate many of the
378 conditions described in humans, are largely mediated by the direct action of melanocortins via
379 MC4R on Kiss1 neurons and not to their obese phenotype. This is because the ablation of MC4R
380 from Kiss1 neurons largely replicated the reproductive impairments observed in MC4RKO female
381 mice without inducing obesity, and the selective reinsertion of MC4R into Kiss1 neurons of
382 MC4RKO mice significantly improved their reproductive function without changing their obese
383 phenotype. Strikingly, puberty onset was advanced in Kiss1-MC4RKO females. Our findings
384 revealed a low melanocortin tone in the hypothalamus of females during pubertal development,
385 characterized by lower levels of *Agrp, Mc4r* and *Mc3r* expression at the time of puberty onset
386 (~PND30). This developmental decline in the expression of melanocortin receptors is in line with
387 the advanced timing of puberty onset in females when MC4R is congenitally ablated from Kiss1
388 neurons. A recent study using whole body MC3RKO mice showed a trend to delayed puberty
389 onset in both sexes (38), suggesting that MC3R, which is also expressed in Kiss1 neurons, may
390 be more critical for the timing of puberty onset in males. However, in females the combination of
391 MC3R and MC4R action may be necessary for pubertal development. Interestingly, the Kiss1-
392 MC4RKO and *Kiss1-cre:MC4R-LoxTB* mice do not show an advancement in puberty onset as we
393 observed in Kiss1-MC4RKO mice; however, these mice show a significant increase in body
394 weight at the time of puberty onset already. We can therefore speculate that the increased
395 adiposity is masking the specific effect of MC4R ablation from Kiss1 neurons on puberty, that we
396 see in the non-obese Kiss1-MC4RKO female mice. Our findings presented in this study do not
397 rule out the existence of additional sites of action of MC4R in other neuronal populations to

398 regulate reproduction, *e.g.,* GnRH neurons, which also express *Mc4r* (17, 22). Indeed, the lack of
399 full recovery of the reproductive function in *Kiss1-cre:MC4R-LoxTB* mice suggests that MC4R in
400 Kiss1 neurons is necessary but not sufficient to achieve full reproductive capabilities.
401 In addition to early puberty onset, Kiss1-MC4RKO females displayed an impaired preovulatory
402 LH surge driving ovulation and had fewer corpora lutea in their ovaries compared to control
403 littermates, further supporting a role of MC4R in regulating ovulation. In adulthood, the
404 reproductive phenotype observed in Kiss1-MC4RKO and MC4R-loxTB female mice (increased
405 LH, irregular estrous cycles, oligo-ovulation, increased cystic follicles) correlates with the
406 phenotype observed in PCOS mouse models (19, 20). In fact, an association between *MC4R*
407 mutations and PCOS has been reported in patients (9). However, our mouse models failed to
408 display higher levels of circulating androgens or AMH, two of the hallmarks of PCOS (21),
409 suggesting that melanocortin signaling is unlikely to be a main contributing factor in the
410 development of this syndrome.
411 Our data revealing early puberty onset and impaired LH pulse and surge driving ovulation support
412 a direct role of MC4R on the two primary Kiss1 populations regulating these functions (ARH and
413 AVPV/PeN). We further investigated this and found that MC4R signaling excites Kiss1^{ARH} neurons
414 and inhibits Kiss1$^{AVPV/PeN}$ neurons in an estradiol-dependent manner. In Kiss1^{ARH} neurons, bath
415 applied or optogenetically-evoked release of melanocortin agonists induce a direct excitatory
416 inward current. Our studies using whole cell voltage clamp in female mice were able to detect a
417 melanocortin-mediated inward current in Kiss1^{ARH} neurons that would increase excitability.
418 Previously, an MCR-activation effect was not detected in cell-attached recordings of diestrus
419 females (13). However, cell-attached recordings do not measure a direct response in isolated
420 Kiss1^{ARH} neurons but rather the summation of multiple synaptic inputs to Kiss1^{ARH} neurons. Most
421 importantly, we did not see a difference in the excitatory response in synaptically isolated Kiss1^{ARH}
422 neurons from E2-treated versus vehicle-treated females. This emphasizes the importance of
423 doing whole-cell recording from isolated Kiss1 neurons. The modulatory actions of POMC^{ARH}

424 neuronal projections to Kiss1^{ARH} neurons can also occur through a) the excitatory action of
425 glutamate in a process that is facilitated in the presence of estradiol, in line with previous
426 publications (15, 39), and b) the inhibitory action of β-endorphin, suggesting that POMC^{ARH}
427 neurons are able to exert a precise regulatory role of the GnRH pulse generator, *i.e.* Kiss1^{ARH}
428 neurons, in response to metabolic challenges. In the AVPV/PeN, MC4R agonists inhibited
429 Kiss1$^{AVPV/PeN}$ neurons in an estradiol-dependent manner, which utilized a Gα_q-coupled membrane
430 estrogen receptor (STX receptor) to attenuate the inhibitory tone of MC4R in these neurons. To
431 date, two instances of MC4R-mediated inhibition have been described in the central nervous
432 system: MC4R can Gi,o couple to open K+ (Kir6.2) channels in parasympathetic preganglionic
433 neurons in the brain stem (33), and MC4R can directly couple to K+ (Kv7.1) channels in the
434 hypothalamic paraventricular nucleus neurons (40). Based on the robust αMSH labeling, we
435 believe that POMC projections represent a significant input to Kiss1$^{AVPV/PeN}$ neurons. Interestingly,
436 our findings describe an inhibitory role of MC4R in the reproductive neuroendocrine axis. This
437 steroid state dependent effect is particularly relevant because in the context of reproduction, the
438 two populations of Kiss1 neurons are strikingly different in their response to estradiol, where
439 Kiss1^{ARH} and Kiss1$^{AVPV/PeN}$ neurons are inhibited or stimulated, respectively, in order to mount the
440 negative versus positive feedback of sex steroids (16). This differential regulation allows for the
441 episodic versus surge release of GnRH; however, the cellular mechanisms underlying these
442 opposing roles of Kiss1 neurons to the same stimulus, *i.e.* circulating E2 levels, remain unknown.
443 Although there were no differences in the magnitude of the electrophysiological responses to
444 MTII in Kiss1^{ARH} neurons in vehicle- versus E2-treated, ovariectomized females, we cannot rule
445 out that E2 affects other systems activated by the MC4R signaling cascade as recently reported
446 in MC4R expressing neurons of the ventromedial nucleus (VMH) (41). Interestingly, puberty onset
447 was advanced in Kiss1-MC4RKO females. This data suggests that the inhibitory tone of MC4R
448 signaling on Kiss1$^{AVPV/PeN}$ neurons might also be involved in the timing of puberty onset, which in
449 turn suggests a role for this female-specific population of Kiss1 neurons in sexual maturation. This

450 phenomenon could explain the earlier age of puberty onset frequently seen in females of most
451 mammalian species compared to their male counterparts (42). Furthermore, our findings suggest
452 that metabolic cues, through the regulation of the melanocortin output onto Kiss1$^{AVPV/PeN}$ neurons,
453 are essential for the timing and magnitude of the GnRH/LH surge. Future studies are warranted
454 to fully elucidate synaptic input and postsynaptic cascades in the POMC-Kiss1$^{AVPV/PeN}$ circuit.
455 Altogether, our data reveal a differential regulatory action of MC4R in the neural control of GnRH
456 release, participating in both the surge (E2-treated, ovariectomized female) and the pulse-like
457 (ovariectomized female) modes of LH release through the cellular regulation of Kiss1 neurons
458 (**Fig. 6**), which translate into our findings on the conditional knockout of *Mc4r* from Kiss1 neurons.
459 These findings are important because the reproductive abnormalities often attributed to obesity
460 in MC4R deficient patients may not be caused by the excess in body weight but, at least in part,
461 by a deficiency in MC4R signaling directly at the level of Kiss1 neurons that affects predominantly
462 the ability to mount a preovulatory LH surge.
463

464 **Materials and Methods:**

465 Detailed description of the materials and methods used in this study are given in ***SI Appendix***.
466

467 **Figure legends:**

468 **Fig. 1. *Mc4r* is expressed within Kiss1 neurons and determines the timing of puberty onset.**
469 **(A)** *In situ* hybridization using RNAscope technology showed co-expression of *Kiss1* (green) and
470 *Mc4r* (red) mRNA transcripts within ARH neurons cell bodies of ovariectomized female mice
471 (n=4). *Kiss1* and *Mc4r mRNAs* were co-expressed above background threshold levels within
472 84.01% of ARH cell bodies. Scale bar is 100 µm. **(B)** RNAscope in the AVPV/PeN of OVX+ E2
473 treated females (n=4/group) shows co-expression of *Kiss1* (green) and *Mc4r* (red) mRNA

474 transcripts within AVPV/PeN neurons. *Kiss1* and *Mc4r* mRNAs are co-expressed above
475 background threshold levels within 74.06% AVPV/PeN cell bodies. Scale bar is 100 μm.
476 Kiss1-MC4RKO females display advanced puberty onset, assessed by daily monitoring of vaginal
477 opening **(C)** and first estrus **(D)**, as documented by cumulative percent and mean age of animals
478 at vaginal opening **(C)** and first estrus **(D)** in Kiss1-MC4RKO females (n=24) compared to WT
479 littermates (n=19). *p<0.05 by Student's t-test. Data presented as the mean± SEM. **(E)** Female
480 Kiss1-MC4RKO (n=19) have normal body weight at the time of puberty onset compared to their
481 WT littermates (n=15). **(F)** Ontogeny expression of melanocortin genes (*Agrp*, *Pomc*, *Mc4r and*
482 *Mc3r*) in the ARH of WT female mice at different postnatal pre-pubertal and pubertal ages: P10,
483 P15, P22 and P30, normalized to the housekeeping gene *Hprt*. (*n values*: females at P10 (n=6),
484 P15 (n=6), P22 (n=6), and P30 (n=5)). Groups with different letters are significantly different
485 (p<0.05), as determined by one-way ANOVA followed by the Student-Newman-Keuls test. Data
486 presented as the mean± SEM.
487
488 **Fig. 2. Deletion of MC4R from Kiss1 neurons impairs fertility in Kiss1-MC4RKO females.**
489 **(A)** Female Kiss1-MC4RKO (n=19) have normal body weight from weaning and until post-natal
490 day (PND) 150 compared to their WT littermates (n=15). **(B)** Representative examples of estrous
491 cycles in Kiss1-MC4RKO and control females (n=5/group) assessed by daily vaginal cytology for
492 15 days. **(C)** Kiss1-MC4RKO females displayed irregular estrous cycles with a longer time in
493 diestrus and a shorter time in estrus compared to control females. *** P < 0.001 Two-way ANOVA.
494 **(D)** Pattern of LH pulsatility was analyzed in gonad intact Kiss1-MC4RKO (n=6) and control (n=7)
495 females. # Represents LH pulses. **(E)** LH total secretory mass assessed by area under the curve
496 (AUC), **(F)** LH pulse amplitude, **(G)** Basal LH and **(H)** total number of pulses /180 min were
497 analyzed. *p<0.05 by Student's t-test. The expression of the KNDy genes *Pdyn* **(I)**, *Kiss1* **(J)**,
498 *Tac2* **(K)** and *Tacr3* **(L)**, was assessed in the ARH of adult Kiss1-MC4RKO (n=6) and control
499 (n=3) females. **p<0.01 by Student's t-test. Data presented as the mean± SEM. **(M)** Kiss1-

500 MC4RKO (n=6) and control (n=5) females were subjected to an LH surge induction protocol. LH
501 samples were collected in the morning (AM [8 a.m.]) and evening (PM [7 p.m.]) after lights off. **P
502 < 0.01, Two-way ANOVA followed by Bonferroni *post hoc* test. **(N)** Ovarian histology shows a
503 decrease in the number of corpora lutea (CL, **O**) and increase in the number of cystic follicles
504 (CF, **P**) of Kiss1-MC4RKO compared to controls(n=5/group). # represents cystic follicles. Serum
505 levels of Testosterone **(Q)** and AMH **(R)** in adult gonad intact Kiss1-MC4RKO and control females
506 (n=5/group). Student t test for unpaired samples. Data presented as the mean± SEM. Kiss1-
507 MC4RKO females display impaired fertility characterized by increased time to deliver pups **(S)**
508 and decreased number of pups per litter **(T)**, (n=9/group). *p<0.05 by Student's t-test. Data
509 presented as the mean± SEM.
510
511 **Fig. 3. Re-insertion of MC4R in Kiss1 neurons restores estrous cyclicity and LH pulsatility**
512 **in Kiss1-cre:MC4R-LoxTB females.**
513 **(A)** *Kiss1-cre*:MC4R-LoxTB (n=11) and MC4R-loxTB (MC4RKO) (n=7) displayed normal puberty
514 onset as compared to their control littermates (n=14), as documented by cumulative percent and
515 mean age of animals at vaginal opening and first estrus. **(B)** *Kiss1-cre*:MC4R-LoxTB and MC4R-
516 loxTB both had significantly higher body weights at the time of puberty onset compared to their
517 controls. **P < 0.01, *** P < 0.001 by one way ANOVA. **(C)** MC4R-loxTB (n=7) and *Kiss1-*
518 *cre*:MC4R-LoxTB (n=11) females displayed significantly higher body weight than their littermates
519 (n=10) from post-natal day 30 onwards, *p<0.05 and **P < 0.01. Data presented as the mean±
520 (SEM). **(D)** Representative examples of estrous cycles of MC4R-loxTB (n=4), *Kiss1-cre*:MC4R-
521 LoxTB (n=5) and control littermate mice, (n=4) assessed by daily monitoring of vaginal smears for
522 15 days. (D/M: diestrus/metestrus, P: proestrus, E: estrus). **(E)** MC4R-loxTB females displayed
523 irregular estrous cycles, presenting longer time in diestrus and shorter time in estrus compared
524 to control females, while *Kiss1-cre*:MC4R-LoxTB females displayed regular estrous cyclicity,
525 similar to controls. *p<0.05, **P < 0.01, *** P < 0.001, ****P < 0.0001, Two-way ANOVA. Data

526 presented as the mean± SEM. **(F)** Pattern of LH pulsatility analyzed in gonad intact MC4R-loxTB
527 (n=4), *Kiss1-cre*:MC4R-LoxTB (n=5) and control littermates females (n=5). LH samples were
528 collected every 10 min for 180 minutes; # represents LH pulses. **(G)** LH total secretory mass, **(H)**
529 LH pulse amplitude, **(I)** basal LH, and **(J)** total number of pulses /180 min were assessed. *p<0.05,
530 **P < 0.01 by one way ANOVA. **(K)** Representative samples of ovarian histology from MC4R-
531 loxTB, *Kiss1-cre*:MC4R-LoxTB and control females (n=5/group); CL: Corpora lutea. Data are
532 presented as the mean± SEM. **(L)** Ovarian histology showed a significant decrease in the number
533 of corpora lutea in the MC4RKO and *Kiss1-cre*:MC4R-LoxTB compared to controls. Groups with
534 different letters are significantly different. Serum levels of **(M)** Testosterone and **(N)** AMH in adult
535 gonad intact females MC4R-loxTB, *Kiss1-cre*:MC4R-LoxTB and their control littermates. *p<0.05,
536 ****P < 0.0001, One Way ANOVA. Data are presented as the mean± SEM.
537
538 **Fig. 4. Kiss1^{ARH} neurons are activated by melanocortin agonists and respond to**
539 **optogenetic stimulation of POMC neurons.**
540 **(A)** Slices were taken from *Kiss1-cre* injected (confocal image) brains to target fluorescent cells
541 (arrowhead) for recording (white outline over electrode). **(B)** Whole cell voltage clamp recording
542 of Kiss1^{ARH} neurons following the direct application of the high affinity melanocortin receptor
543 agonist melanotan II (MTII, 250 nM) was added directly to the bath and the response was
544 compared between slices from OVX and OVX+E females. **(C)** While the average inward current
545 was slightly higher in the OVX+E state, this was not a significant difference (Student's t-test for
546 unpaired samples, p>0.05). **(D)** The MC4R-selective agonist THIQ (100 nM) was perfused, and
547 excitatory inward currents were generated in Kiss1^{ARH} neurons. **(E)** Images are of AAV-driven
548 labeling of POMC cells as seen through the confocal. **(F)** Using the AAV-driven expression of
549 channelrhodopsin in adult *Pomc-cre* mice, high frequency stimulation elicited a slow inward
550 current in Kiss1 neurons. **(G)** The identity of cells was confirmed through the presence of a
551 persistent sodium current (see (23)) and/or with RT-PCR of harvested cytoplasm showing *Kiss1*

552 expression. (Gel: MM=molecular marker, TC=tissue controls). **(H)** A direct synaptic projection
553 from POMC to Kiss1^{ARH} neuron (*posthoc* identified) was confirmed using the "rescue" protocol: 1,
554 baseline glutamatergic responses were initially generated (black trace); 2, then action potentials
555 were eliminated by blocking voltage-gated sodium channels with TTX and the postsynaptic
556 response (red trace); 3, blockade of potassium channels facilitated calcium entry into the terminal
557 through ChR2 to release synaptic vesicles, "rescuing" the postsynaptic glutamate response
558 (green trace). **I)** Glutamatergic responses were also often observed, particularly in the ventral
559 ARH. As seen when targeting low input resistance neurons (i.e., Kiss1^{ARH}) with low frequency
560 optogenetic stimulation (5 ms pulse, 50 ms inter-spike interval), the first response in OVX +
561 vehicle females was larger relative to the second response in OVX + E2- treated female mice.
562 Representative traces are the average of 30 sweeps. **(J)** The averaged paired-pulse ratio was
563 lower in recordings from estradiol-treated female mice, indicating an increased release probability
564 (Students t-test $p<0.05$,). **(K)** High frequency optogenetic stimulation elicited a small inward
565 current. **(L)** In a different cell, a high frequency inward current was noted before constant perfusion
566 of SHU9119 for 15 minutes (break between traces). When the stimulation protocol was repeated,
567 no inward current was elicited. **(M)** The majority of high frequency responses were inward and
568 only twice was an inhibitory outward current recorded in identified Kiss1^{ARH} neurons. Perfusion of
569 the non-selective opioid receptor antagonist naloxone reversed the current, eliminating MCR-
570 activation as the mechanism.
571
572 **Fig. 5. Kiss1$^{AVPV/PeN}$ neurons are inhibited by MC4R agonists in an E2-dependent manner.**
573 **(A)** Immunohistochemistry showing typical labeling of α-MSH fibers in the AVPV/PeN region in
574 OVX+E2 WT female mice. **(B)** Whole-cell voltage clamp recordings were made in ChR2-YFP
575 positive cells in brain slices taken from *Kiss1-cre*:Ai32 female mice. Bath application of melanotan
576 II (MTII, 500 nM) generated an inhibitory outward current in a Kiss1$^{AVPV/PeN}$ neuron from OVX
577 female. As the cell was synaptically isolated using bath-applied tetrodotoxin (TTX, 1 μM) this

578 represents a direct effect. Washout of MTII while still in TTX quickly led to a return to baseline
579 RMP. **C)** An IV relationship was plotted using voltage steps before and after MTII administration.
580 The crossing near -85 mV (~EK^+) suggested the opening of a K+ channel. **D)** In a subset of
581 recordings from OVX brains slices, the selective membrane estrogen receptor (Gq-mER) agonist
582 STX (10 nM) was added to the bath for ~10 minutes prior to addition of MTII. STX pretreatment
583 resulted in either a greatly attenuated outward current or even an inward current as shown in this
584 example. **(E)** The mean outward current was significantly higher when recording in $Kiss1^{AVPV/Pen}$
585 neurons from brain slices from vehicle-treated, OVX females compared to E2-treated, OVX
586 females or acute STX-treated brain slices from OVX females (One-way ANOVA $F_{(2,19)}$=12.32,
587 p<0.001; Holm-Sidak *posthoc* comparisons found significant differences between all groups; *
588 p<0.05, *** p<0.001). **(F)** There was no difference in the frequency of mEPSCs after MTII,
589 calculated as a percent of baseline between groups. **(G)** However, there was a significant
590 difference in the mEPSC amplitude (calculated as a percent of baseline) between all groups: main
591 effect $F_{(2,19)}$ =10.58, p<0.001. *Posthoc* comparisons using Holm-Sidak found OVX+STX to be
592 different from both OVX (p<0.001) and OVX+E (p<0.05).
593
594 **Fig. 6. Working model of POMC to Kiss1 neuronal circuitry.**
595 In ovariectomized females, POMC neurons excite $Kiss1^{ARH}$ neurons via glutamate and αMSH
596 release, which activate glutamatergic ionotropic and MC4R, respectively. E2-treatment enhances
597 the glutamatergic excitation of these neurons. In contrast in ovariectomized females, αMSH fibers
598 project to the AVPV/PeN, and MC4R agonists (*i.e.*, MTII) inhibit $Kiss1^{AVPV/PeN}$ neurons via opening
599 a K^+ channel. However, E2-treatment rapidly abrogates (uncouples) the inhibitory MC4R
600 signaling in $Kiss1^{AVPV/PeN}$ neurons, allowing greater excitatory actions of $Kiss1^{ARH}$ neurons via
601 enhanced glutamate release (26).
602
603

604 **Fig. S1. Validation of Kiss-MC4RKO mouse model, related to figure 5.**

605 **(A)** Representative images depicting co-expression of *Kiss1* and *Mc4r* mRNA, using RNAscope,
606 in OVX WT female mice (upper left panel), and OVX Kiss1-MC4RKO female mice (upper right
607 panel). As expected, *Mc4r* was not detected within Kiss1 neurons in Kiss1-MC4RKO females. **(B)**
608 Representative images depicting comparable *Mc4r* mRNA expression in the paraventricular
609 hypothalamus between OVX WT and Kiss1-MC4RKO females. Scale bar is 100 μm.

610

611 **Fig. S2. Validation of Kiss1-cre:MC4R-LoxTB mouse model, related to figure 4.**

612 **(A)** Representative images depicting co-expression of *Kiss1* and *Mc4r* mRNA, using RNAscope,
613 in OVX *Kiss1-cre:MC4R-LoxTB* female mice in the ARH (upper right panel). As expected, Mc4r
614 is detected within Kiss1 neurons in *Kiss1-cre*:*MC4R-LoxTB* females. **(B)** Representative images
615 depicting the absence of *Mc4r* mRNA expression in the paraventricular hypothalamus of *Kiss1-*
616 *cre*:MC4R-LoxTB female, compared to their WT control littermates. Scale bar is 100 μm.

617

618

619 **Acknowledgments:**

620 The authors would like to recognize the excellent technical expertise of Ms. Martha A. Bosch
621 (tissue preparation, immunohistochemical procedure and single cell RT-PCR of recorded
622 neurons). In addition, we thank Dr. Rona Carroll for her assistance at Harvard Medical School
623 and Mr. Cole Martinson, a student worker in the Ronnekleiv/ Kelly laboratories, for his assistance
624 with genotyping and care of mouse colonies at OHSU. The University of Virginia Center for
625 Research in Reproduction Ligand Assay and Analysis Core is supported by the Eunice Kennedy
626 Shriver NICHD/NIH (NCTRI) Grant P50-HD28934. This work was supported by PHS MPI grant
627 DK68098 to MJK and OKR; HD090151, HD099084 and DK133760 to VMN, and The Charles A.
628 King Trust Postdoctoral Research Fellowship Award, The Lalor Foundation Postdoctoral
629 Fellowship Award, the Women's brain initiative Fellowship Award, the ROSA SCORE pilot grant

(supported by NIH Research Grant U54 AG062322 funded by The National Institute on Aging (NIA) and Office of Research on Women's Health (ORWH)) and the IBRO-ISN Research Fellowship Award to RT, and startup funds from Appalachian State University to TLS.

References:

1. U. Health (2020) Infertility.
2. M. L. Andermann, B. B. Lowell, Toward a Wiring Diagram Understanding of Appetite Control. *Neuron* **95**, 757-778 (2017).
3. R. D. Cone, Studies on the physiological functions of the melanocortin system. *Endocr Rev* **27**, 736-749 (2006).
4. B. P. Shah *et al.*, MC4R-expressing glutamatergic neurons in the paraventricular hypothalamus regulate feeding and are synaptically connected to the parabrachial nucleus. *Proceedings of the National Academy of Sciences of the United States of America* **111**, 13193-13198 (2014).
5. K. Wang *et al.*, Neuroanatomy of melanocortin-4 receptor pathway in the mouse brain. *Open Life Sci* **15**, 580-587 (2020).
6. I. S. Farooqi *et al.*, Clinical spectrum of obesity and mutations in the melanocortin 4 receptor gene. *The New England journal of medicine* **348**, 1085-1095 (2003).
7. I. A. Hainerová, H. Zamrazilová, D. Sedláčková, V. Hainer, Hypogonadotropic hypogonadism in a homozygous MC4R mutation carrier and the effect of sibutramine treatment on body weight and obesity-related health risks. *Obes Facts* **4**, 324-328 (2011).
8. M. Doulla, A. D. McIntyre, R. A. Hegele, P. H. Gallego, A novel MC4R mutation associated with childhood-onset obesity: A case report. *Paediatr Child Health* **19**, 515-518 (2014).
9. A. A. Batarfi *et al.*, MC4R variants rs12970134 and rs17782313 are associated with obese polycystic ovary syndrome patients in the Western region of Saudi Arabia. *BMC Med Genet* **20**, 144 (2019).
10. X. Chen *et al.*, Deficient melanocortin-4 receptor causes abnormal reproductive neuroendocrine profile in female mice. *Reproduction (Cambridge, England)* **153**, 267-276 (2017).
11. M. Sandrock *et al.*, Reduction in corpora lutea number in obese melanocortin-4-receptor-deficient mice. *Reprod Biol Endocrinol* **7**, 24 (2009).
12. L. Cui *et al.*, Dapagliflozin partially restores reproductive function in MC4R KO obese female mice. *The Journal of endocrinology* **254**, 65-76 (2022).
13. M. Manfredi-Lozano *et al.*, Defining a novel leptin-melanocortin-kisspeptin pathway involved in the metabolic control of puberty. *Mol Metab* **5**, 844-857 (2016).
14. C. C. Nestor *et al.*, Optogenetic Stimulation of Arcuate Nucleus Kiss1 Neurons Reveals a Steroid-Dependent Glutamatergic Input to POMC and AgRP Neurons in Male Mice. *Mol Endocrinol* **30**, 630-644 (2016).
15. J. Qiu *et al.*, Estrogenic-dependent glutamatergic neurotransmission from kisspeptin neurons governs feeding circuits in females. *Elife* **7** (2018).

16. R. L. Goodman, A. E. Herbison, M. N. Lehman, V. M. Navarro, Neuroendocrine control of gonadotropin-releasing hormone: Pulsatile and surge modes of secretion. *Journal of neuroendocrinology* **34**, e13094 (2022).
17. D. D. Israel *et al.*, Effects of leptin and melanocortin signaling interactions on pubertal development and reproduction. *Endocrinology* **153**, 2408-2419 (2012).
18. M. Manfredi-Lozano, J. Roa, M. Tena-Sempere, Connecting metabolism and gonadal function: Novel central neuropeptide pathways involved in the metabolic control of puberty and fertility. *Front Neuroendocrinol* **48**, 37-49 (2018).
19. A. M. Moore, M. Prescott, R. E. Campbell, Estradiol negative and positive feedback in a prenatal androgen-induced mouse model of polycystic ovarian syndrome. *Endocrinology* **154**, 796-806 (2013).
20. E. A. McCarthy *et al.*, Inhibiting Kiss1 Neurons With Kappa Opioid Receptor Agonists to Treat Polycystic Ovary Syndrome and Vasomotor Symptoms. *J Clin Endocrinol Metab* **107**, e328-e347 (2022).
21. D. Dewailly, A. L. Barbotin, A. Dumont, S. Catteau-Jonard, G. Robin, Role of Anti-Müllerian Hormone in the Pathogenesis of Polycystic Ovary Syndrome. *Frontiers in endocrinology* **11**, 641 (2020).
22. J. Roa, A. E. Herbison, Direct regulation of GnRH neuron excitability by arcuate nucleus POMC and NPY neuron neuropeptides in female mice. *Endocrinology* **153**, 5587-5599 (2012).
23. C. Zhang, M. A. Bosch, J. Qiu, O. K. Ronnekleiv, M. J. Kelly, 17beta-Estradiol increases persistent Na(+) current and excitability of AVPV/PeN Kiss1 neurons in female mice. *Mol Endocrinol* **29**, 518-527 (2015).
24. J. D. Clements, G. L. Westbrook, Activation kinetics reveal the number of glutamate and glycine binding sites on the N-methyl-D-aspartate receptor. *Neuron* **7**, 605-613 (1991).
25. T. L. Stincic, P. Grachev, M. A. Bosch, O. K. Rønnekleiv, M. J. Kelly, Estradiol drives the anorexigenic activity of proopiomelanocortin neurons in female mice. *eNeuro* **5**, e0103-0118.2018 (2018).
26. J. Qiu *et al.*, High-frequency stimulation-induced peptide release synchronizes arcuate kisspeptin neurons and excited GnRH neurons. *eLife* **5**, e16246 (2016).
27. J. Qiu *et al.*, Estrogenic-dependent glutamatergic neurotransmission from kisspeptin neurons governs feeding circuits in females. *eLife* **7**, e35656 (2018).
28. T. L. Stincic, J. Qiu, A. M. Connors, M. J. Kelly, O. K. Rønnekleiv, Arcuate and Preoptic Kisspeptin neurons exhibit differential projections to hypothalamic nuclei and exert opposite postsynaptic effects on hypothalamic paraventricular and dorsomedial nuclei in the female mouse. *eneuro* 10.1523/eneuro.0093-21.2021, ENEURO.0093-0021.2021 (2021).
29. M. A. Herman, F. Ackermann, T. Trimbuch, C. Rosenmund, Vesicular glutamate transporter expression level affects synaptic vesicle release probability at hippocampal synapses in culture. *The Journal of Neuroscience* **34**, 11781-11791 (2014).
30. J. E. Thornton, M. D. Loose, M. J. Kelly, O. K. Rønnekleiv, Effects of estrogen on the number of neurons expressing β-endorphin in the medial basal hypothalamus of the female guinea pig. *The Journal of comparative neurology* **341**, 68-77 (1994).

31. K. G. Mountjoy, M. T. Mortrud, M. J. Low, R. B. Simerly, R. D. Cone, Localization of the melanocortin-4 receptor (MC4-R) in neuroendocrine and autonomic control circuits in the brain. *Molecular Endocrinology* **8**, 1298-1308 (1994).
32. J. Yu *et al.*, Determination of the melanocortin-4 receptor structure identifies Ca²⁺ as a cofactor for ligand binding. *Science* **368**, 428-433 (2020).
33. J. W. Sohn *et al.*, Melanocortin 4 receptors reciprocally regulate sympathetic and parasympathetic preganglionic neurons. *Cell* **152**, 612-619 (2013).
34. M. J. Kelly, M. D. Loose, O. K. Ronnekleiv, Estrogen suppresses mu-opioid- and GABAB-mediated hyperpolarization of hypothalamic arcuate neurons. *The Journal of neuroscience : the official journal of the Society for Neuroscience* **12**, 2745-2750 (1992).
35. A. H. Lagrange, O. K. Ronnekleiv, M. J. Kelly, The potency of mu-opioid hyperpolarization of hypothalamic arcuate neurons is rapidly attenuated by 17 beta-estradiol. *The Journal of neuroscience : the official journal of the Society for Neuroscience* **14**, 6196-6204 (1994).
36. J. Qiu *et al.*, Rapid signaling of estrogen in hypothalamic neurons involves a novel G-protein-coupled estrogen receptor that activates protein kinase C. *The Journal of neuroscience : the official journal of the Society for Neuroscience* **23**, 9529-9540 (2003).
37. J. Qiu *et al.*, A G-protein-coupled estrogen receptor is involved in hypothalamic control of energy homeostasis. *The Journal of neuroscience : the official journal of the Society for Neuroscience* **26**, 5649-5655 (2006).
38. B. Y. H. Lam *et al.*, MC3R links nutritional state to childhood growth and the timing of puberty. *Nature* **599**, 436-441 (2021).
39. T. L. Stincic, P. Grachev, M. A. Bosch, O. K. Ronnekleiv, M. J. Kelly, Estradiol Drives the Anorexigenic Activity of Proopiomelanocortin Neurons in Female Mice. *eNeuro* **5** (2018).
40. M. Ghamari-Langroudi *et al.*, G-protein-independent coupling of MC4R to Kir7.1 in hypothalamic neurons. *Nature* **520**, 94-98 (2015).
41. W. C. Krause *et al.*, Oestrogen engages brain MC4R signalling to drive physical activity in female mice. *Nature* **599**, 131-135 (2021).
42. N. Brix *et al.*, Timing of puberty in boys and girls: A population-based study. *Paediatr Perinat Epidemiol* **33**, 70-78 (2019).

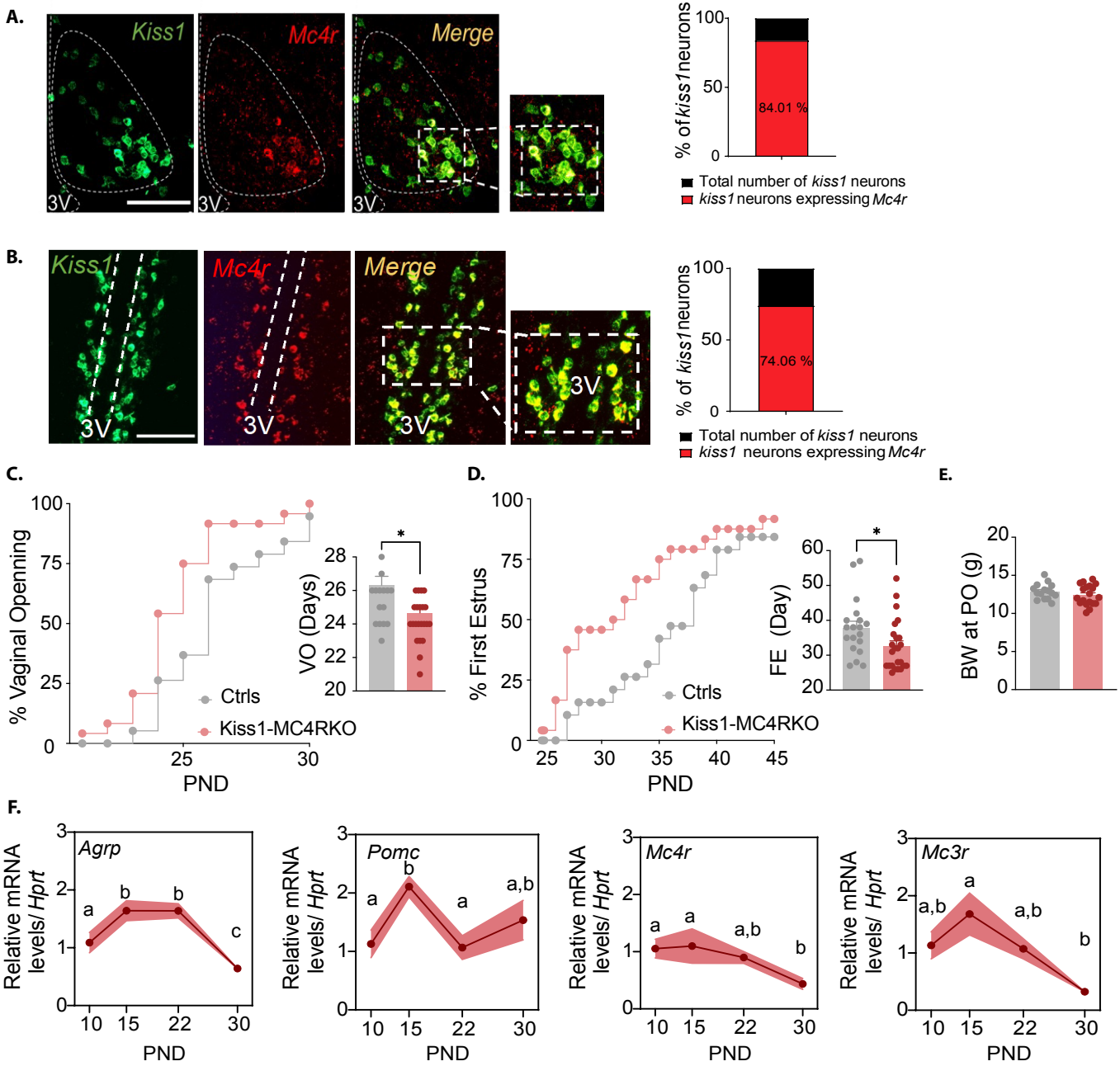
A.
Kiss1
Mc4r
Merge
3V
% of kiss1 neurons
84.01 %
Total number of kiss1 neurons
kiss1 neurons expressing Mc4r
B.
74.06 %
C.
% Vaginal Openning
PND
Ctrls
Kiss1-MC4RKO
VO (Days)
D.
% First Estrus
FE (Day)
E.
BW at PO (g)
F.
Agrp
Pomc
Mc4r
Mc3r
Relative mRNA levels/ Hprt

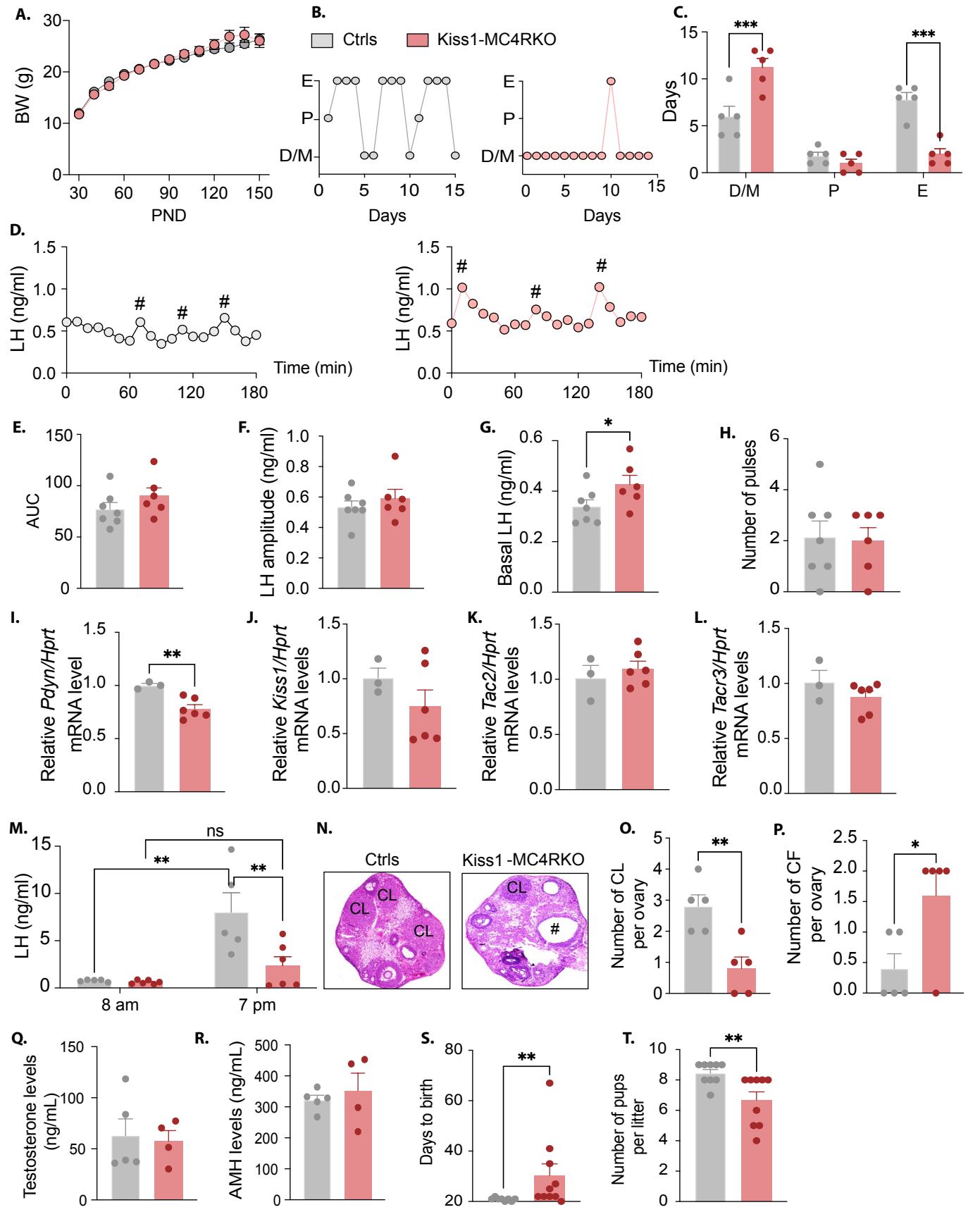
A.
BW (g)
PND
B.
Ctrls
Kiss1-MC4RKO
E
P
D/M
Days
C.
Days
D/M
P
E
***
D.
LH (ng/ml)
Time (min)
#
E.
AUC
F.
LH amplitude (ng/ml)
G.
Basal LH (ng/ml)
*
H.
Number of pulses
I.
Relative Pdyn/Hprt mRNA level
**
J.
Relative Kiss1/Hprt mRNA levels
K.
Relative Tac2/Hprt mRNA levels
L.
Relative Tacr3/Hprt mRNA levels
M.
LH (ng/ml)
ns
**
8 am
7 pm
N.
Ctrls
Kiss1 -MC4RKO
CL
#
O.
Number of CL per ovary
P.
Number of CF per ovary
Q.
Testosterone levels (ng/mL)
R.
AMH levels (ng/mL)
S.
Days to birth
T.
Number of pups per litter

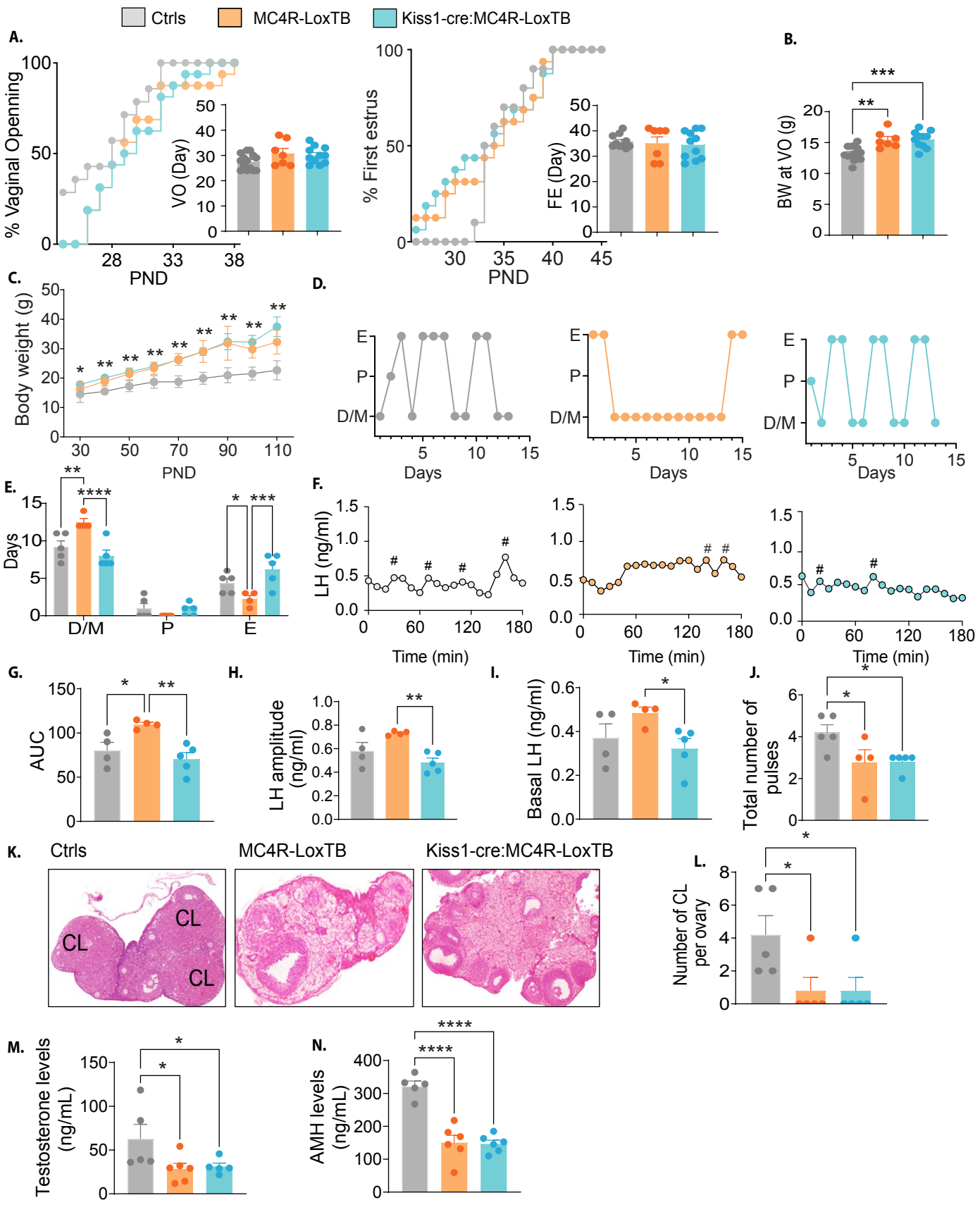
Ctrls
MC4R-LoxTB
Kiss1-cre:MC4R-LoxTB
A.
% Vaginal Openning
PND
VO (Day)
% First estrus
FE (Day)
B.
BW at VO (g)
C.
Body weight (g)
D.
E
P
D/M
Days
E.
Days
D/M
P
E
F.
LH (ng/ml)
Time (min)
G.
AUC
H.
LH amplitude (ng/ml)
I.
Basal LH (ng/ml)
J.
Total number of pulses
K.
Ctrls
MC4R-LoxTB
Kiss1-cre:MC4R-LoxTB
CL
L.
Number of CL per ovary
M.
Testosterone levels (ng/mL)
N.
AMH levels (ng/mL)

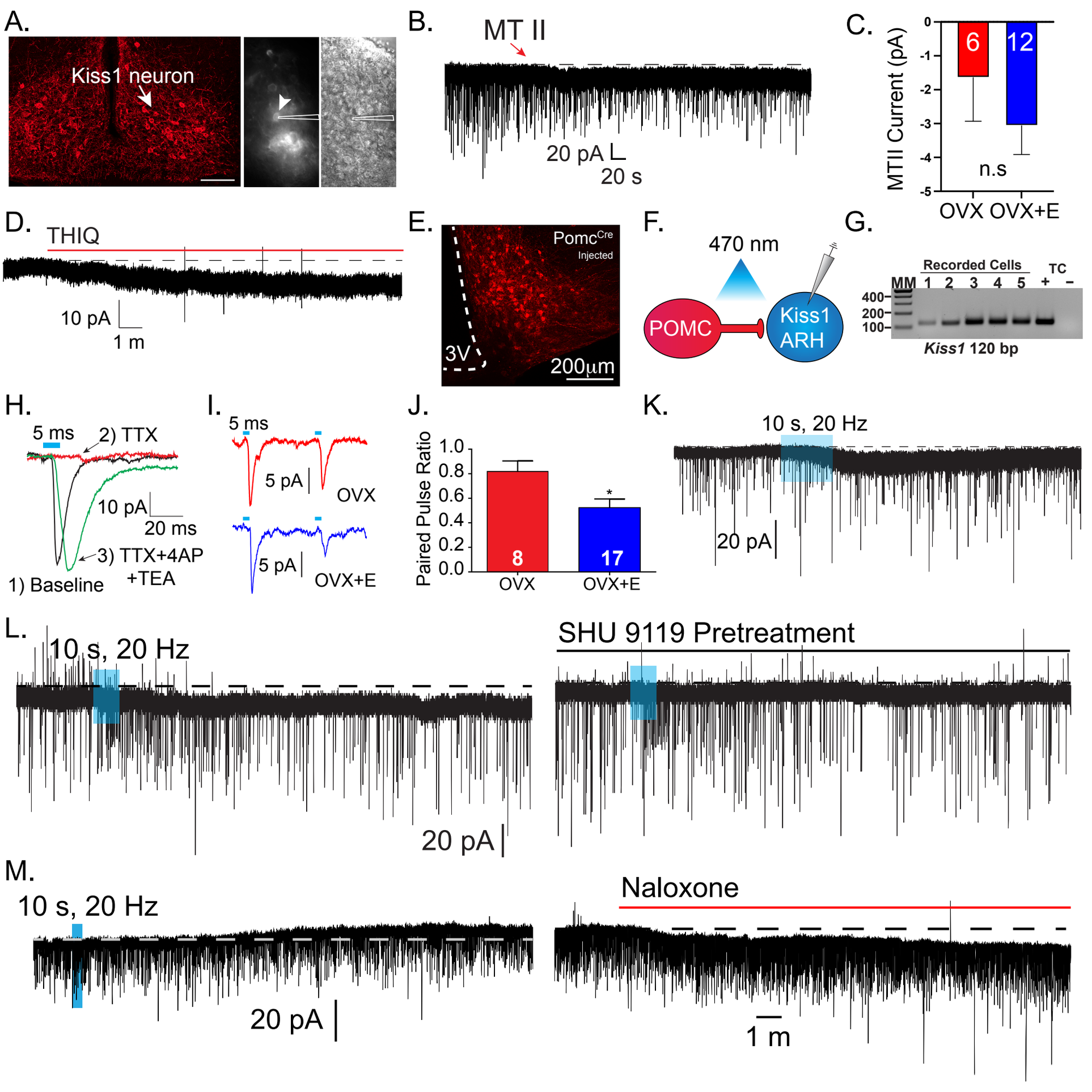
A.
Kiss1 neuron
B.
MT II
20 pA
20 s
C.
MTII Current (pA)
0
-1
-2
-3
-4
-5
6
12
n.s
OVX
OVX+E
D.
THIQ
10 pA
1 m
E.
Pomc^Cre
Injected
3V
200µm
F.
470 nm
POMC
Kiss1
ARH
G.
Recorded Cells
MM
1
2
3
4
5
TC
+
–
400
200
100
Kiss1 120 bp
H.
5 ms
2) TTX
10 pA
20 ms
3) TTX+4AP
+TEA
1) Baseline
I.
5 ms
5 pA
OVX
5 pA
OVX+E
J.
Paired Pulse Ratio
1.0
0.8
0.6
0.4
0.2
0.0
8
17
*
OVX
OVX+E
K.
10 s, 20 Hz
20 pA
L.
10 s, 20 Hz
20 pA
SHU 9119 Pretreatment
M.
10 s, 20 Hz
20 pA
Naloxone
1 m

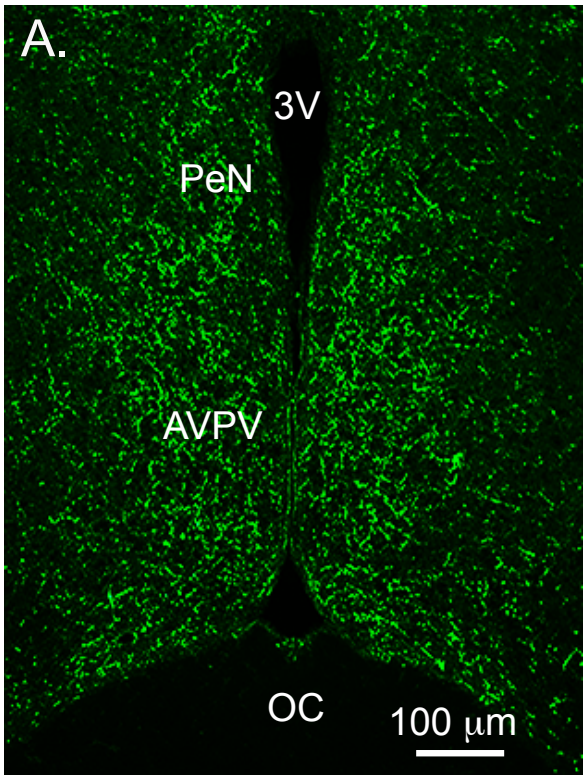
A.
3V
PeN
AVPV
OC
100 µm

anti-αMSH

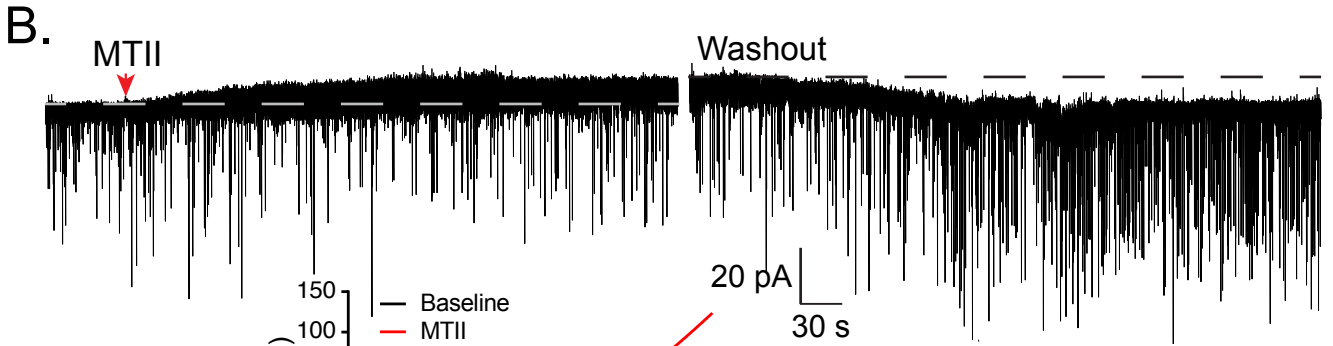
B.
MTII
Washout
20 pA
30 s

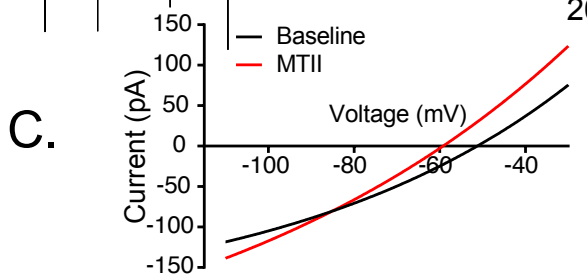
C.
Baseline
MTII
Voltage (mV)
Current (pA)
150
100
50
0
-50
-100
-150
-100
-80
-60
-40

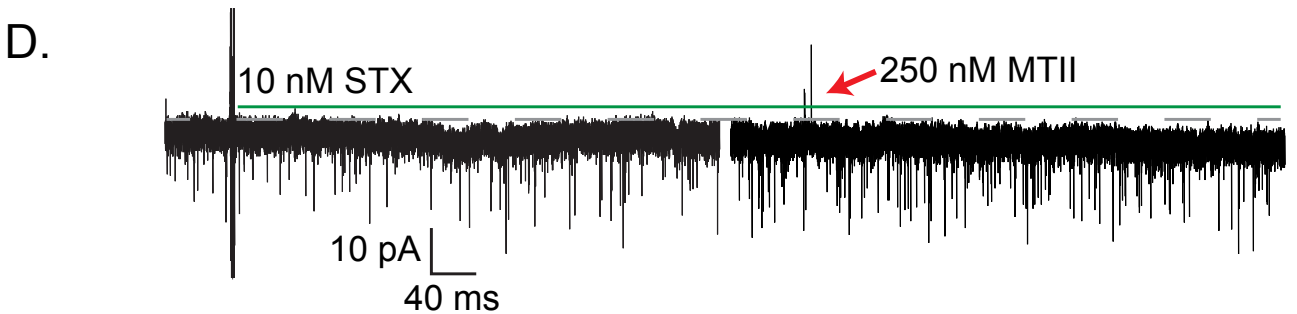
D.
10 nM STX
250 nM MTII
10 pA
40 ms

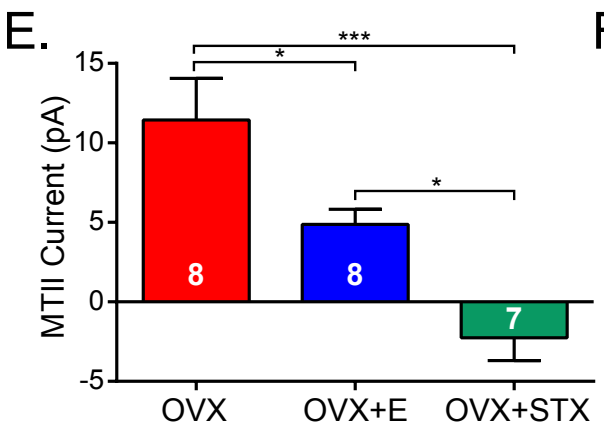
E.
MTII Current (pA)
15
10
5
0
-5
***
*
*
8
8
7
OVX
OVX+E
OVX+STX

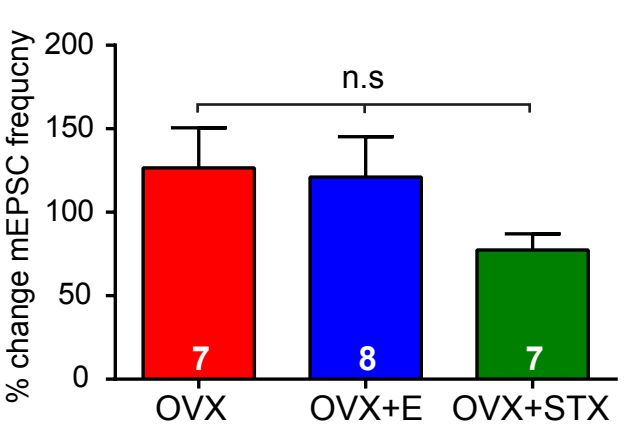
F.
% change mEPSC frequcny
200
150
100
50
0
n.s
7
8
7
OVX
OVX+E
OVX+STX

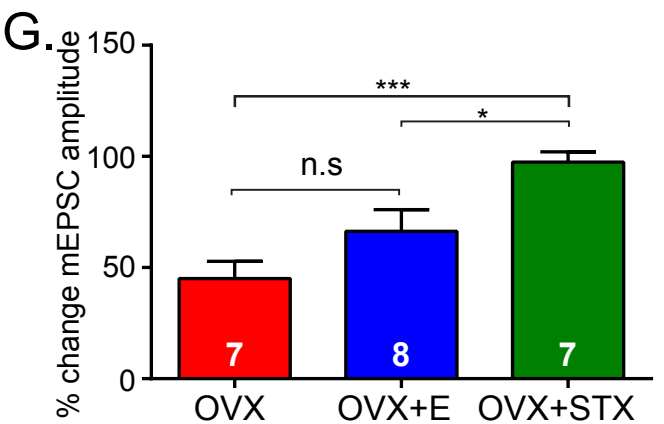
G.
% change mEPSC amplitude
150
100
50
0
***
*
n.s
7
8
7
OVX
OVX+E
OVX+STX

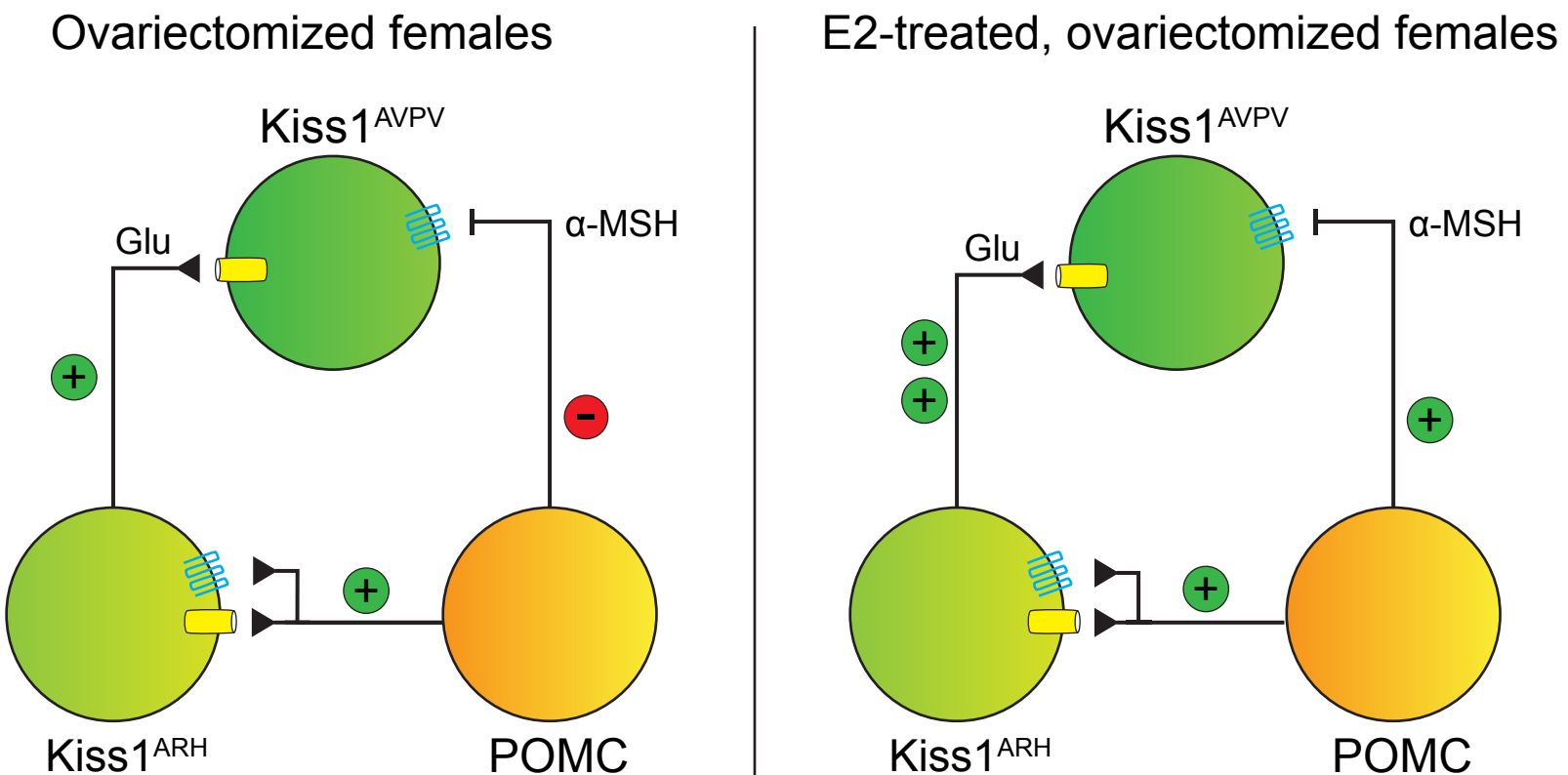
Ovariectomized females
Kiss1AVPV
Glu
α-MSH
+
-
+
Kiss1ARH
POMC
E2-treated, ovariectomized females
Kiss1AVPV
Glu
α-MSH
+
+
+
+
Kiss1ARH
POMC